

Journal of Materials Chemistry C

Accepted Manuscript



This is an *Accepted Manuscript*, which has been through the Royal Society of Chemistry peer review process and has been accepted for publication.

Accepted Manuscripts are published online shortly after acceptance, before technical editing, formatting and proof reading. Using this free service, authors can make their results available to the community, in citable form, before we publish the edited article. We will replace this *Accepted Manuscript* with the edited and formatted *Advance Article* as soon as it is available.

You can find more information about *Accepted Manuscripts* in the [Information for Authors](#).

Please note that technical editing may introduce minor changes to the text and/or graphics, which may alter content. The journal's standard [Terms & Conditions](#) and the [Ethical guidelines](#) still apply. In no event shall the Royal Society of Chemistry be held responsible for any errors or omissions in this *Accepted Manuscript* or any consequences arising from the use of any information it contains.

Metallic carbon allotrope with superhardness: A first-principles prediction

Hongxia Bu^{1,2}, Mingwen Zhao^{1*}, Wenzheng Dong¹, Shuangwen Lu¹, Xiaopeng Wang¹

¹ School of Physics & State Key Laboratory of Crystal Materials, Shandong University, Jinan, Shandong 250100, China

² College of Science and Technology, Shandong University of Traditional Chinese Medicine, College Town of Changqing District, Jinan, Shandong 250355, China

Abstract:

Carbon has abundant allotropes with superhardness, but few of them are metallic. From first-principles calculations, we propose a stable metallic carbon allotrope (Hex-C₂₄) phase with superhardness. The Hex-C₂₄ can be thought of as a superlattice of carbon nanotubes and graphene nanoribbons composed of sp^2 - and sp^3 -hybridized carbon atoms. A possible synthetic route to Hex-C₂₄ from graphyne multilayers is evaluated by calculating the transition states between the two phases. Our calculations show that at the uniaxial pressure of around 25 GPa, the energy barrier of this endothermic transition is estimated to be 0.04 eV atom⁻¹, while at the pressure of 34 GPa, the transition is barrierless for specific initial configurations. The cohesive energy, elastic constants, and phonon frequencies unambiguously confirm the structural stability. The hardness of the Hex-C₂₄ is estimated to be exceeding 44.54 GPa, which is 1/2 of diamond. The Hex-C₂₄ phase is metallic with several bands across the Fermi level. Both mechanical and metallic properties of Hex-C₂₄ are anisotropic.

*Corresponding author, E-mail: zmw@sdu.edu.cn

1. Introduction

One of the greatest challenges in materials design is to identify materials with superhardness because they are not only of great scientific interest, but also of practical importance^{1,2}. The strong covalent compounds of carbon, such as diamond, lonsdaleite³, M-carbon⁴, bct C₄ carbon^{5,6}, W-carbon and Z-carbon⁷⁻⁹, R-carbon and P-carbon¹⁰, X- and Y-carbon¹¹ are expected to be powerful superhard candidates. Most of the superhard materials including these carbon allotropes are insulators or semiconductors¹². While superhard materials with conductivity are quite promising for the uses in petroleum drilling tools, geological exploration, mining engineering, cutting tools, grinding tools and special wear-resistant parts. One important focus has been the search for novel materials with superhardness and conductivity^{13, 14}. Meanwhile carbon exhibits numerous phases with distinct *sp*-, *sp*²- and *sp*³-hybridized bonds, yielding various allotropes such as graphite, diamond, carbyne¹⁵, fullerenes¹⁶, nanotubes¹⁷, graphene¹⁸, graphynes¹⁹, and so on. But the richness of its phase diagram does not end there. In fact, many other structures have been proposed during the past years. Pressure-induced changes of bonding from *sp*² to *sp*³ for graphite, fullerenes, and carbon nanotubes (CNTs) have stimulated considerable scientific interest where high pressure serves as a powerful tool to tune the mechanical and electronic properties of carbon allotropes²⁰. This technique has been applied to investigate a number of carbon allotropes including graphite^{4-6, 8, 10-12, 21}, C₆₀ and its derivatives²²⁻²⁴, and CNTs²⁵⁻²⁸. Attractive physical, chemical, and mechanical properties have been identified in these materials under compression²⁹.

Graphyne, a new layered carbon allotrope, was first designed by inserting two *sp*-hybridized carbon atoms into the *sp*²-*sp*² bonds of graphene forming linear -C≡C- linkages¹⁹. The presence of acetylenic groups introduces a rich variety of optical and electronic properties that are quite different from those of graphite^{19, 30}, e.g., the natural band gap opening due to the asymmetric π bindings. Considerable effort has been devoted to growing this novel material, and numerous monomeric and

oligomeric substructures have already been synthesized³¹⁻³⁴. More excitingly, large-area graphdiyne, which belongs to the same family as graphyne, has recently been successfully grown on the surface of copper via a cross-coupling reaction using hexaethynylbenzene³⁵. The fabrication of graphyne can be greatly expected in the near future, since theoretical work shows that it is energetically more stable than graphdiyne¹⁹. The recent progresses on the fabrication of graphene are also helpful for the realization of this novel carbon allotrope. However, it is noteworthy that the chemical potential of carbon atom in this graphyne is higher than those in graphene and graphite, due to the under-coordinated (*sp*-hybridized) carbon atoms in the acetylenic linkages make these structures less stable than both graphene and graphite^{30,36}. It is therefore naturally expected that under high pressure graphyne multilayers may undergo structural transition to a more stable carbon allotrope as what happened in the formation of diamond from graphite. Theoretical investigations on this structural transition as well as the resulting carbon allotrope are highly desirable, both from the fundamental research standpoint and for its potential applications.

Here, from first-principles calculations, we propose a possible endothermic transition of graphyne to a novel carbon allotrope termed hexagonal carbon with 24 atoms in one unit cell (Hex-C₂₄). Our calculations indicate that at zero pressure the energy barrier of this transition is about 0.21 eV atom⁻¹, and decreases drastically with the increase of pressure. At 25 GPa pressure, the energy barrier becomes 0.04 eV atom⁻¹. This value is much lower than that of the transition of graphite to diamond at ultrahigh pressure (around 0.15 eV atom⁻¹)^{6,37,38}. From an energetic point of view, Hex-C₂₄ is more stable than the parent material (graphyne) by about 0.36 eV atom⁻¹, and comparable to diamond. The calculations of phonon spectrum and elastic constants also confirm the dynamic and mechanical stability of this novel carbon allotrope. The hardness of Hex-C₂₄ evaluated from the present calculations is over 44.54 GPa, which is about half of diamond. More interestingly, in contrast to most of superhard materials with covalent bonds which are either insulating or semiconducting, this Hex-C₂₄ is metallic with several bands across the Fermi level. Such conductive carbon allotrope with superhardness is quite promising for the device

applications under extremely conditions

2. Method and computational details

All calculations were performed within the density functional theory (DFT) implemented in the CASTEP package³⁹. The exchange-correlation functional was treated using a generalized gradient approximation (GGA) according to Perdew-Burke-Ernzerhof⁴⁰. The energy cutoff of the plane-wave basis was taken to be 400 eV. The k -point separation in the Brillouin zone of the reciprocal space was set at 0.02 \AA^{-1} according to the Monkhorst-Pack method⁴¹. The internal coordinates and lattice constant were optimized using the so-called Broyden-Fletcher-Goldfarb-Shanno (BFGS) minimization scheme⁴². The structural relaxation was performed until the total energy, the maximum ionic displacement, the maximum stress, and the maximum ionic Hellmann-Feynman force were less than $5 \times 10^{-6} \text{ eV atom}^{-1}$, $5 \times 10^{-4} \text{ \AA}$, 0.02 GPa, and 0.01 eV \AA^{-1} , respectively. The linear or quadratic synchronous transit (LST/QST) method⁴³ combined with conjugate gradient refinements was adopted for the transition state (TS) search that was implemented in the DMol3 package^{44,45}. To determine if the TS connects to the relevant reactant and product, we performed minimum-energy pathway (MEP) calculations within the nudged elastic band (NEB) method⁴⁶. To evaluate the dynamical stability, we calculated the phonon band structure using the Phonon package⁴⁷ with the forces from VASP calculations^{48,49}.

On the basis of the equilibrium structure, series of incremental stress were applied to the crystal to determine the structural response to the stress. At each step, a desired target-stress component was set to a certain value while other components were kept zero. The lattice vectors and atomic positions were then relaxed simultaneously to obtain the final structures and the corresponding strain. In this way, the ideal strength was obtained as the structure collapses.

3. Results and discussion

The atomic framework of the graphyne monolayer can be viewed as carbon

hexagons interconnected by acetylenic $\text{-C}\equiv\text{C-}$ linkages. Different from graphene that is composed solely of sp^2 -hybridized carbon atoms, graphyne is made up of sp - and sp^2 -hybridized carbon atoms. Sp -hybridization is not energetically preferable for the carbon atom. Thus, it is not surprising that graphyne is less stable than graphene and graphite. Our first-principles calculations indicate that the graphyne monolayer is less stable than graphene by about $0.84 \text{ eV atom}^{-1}$, which is in good agreement with previously reported theoretical models^{19,36}. Driven by the high chemical potential of carbon atoms, especially the sp -hybridized carbon atoms, graphyne multilayers may have a strong tendency to bond together via interlayer covalent bonds instead of weak van der Waals interactions and form more stable structures under certain conditions, e.g. high pressure. Analogous to the formation of diamond from graphite, we proposed that a novel carbon allotrope can be generated by compressing graphyne multilayers.

Carbon atoms in a basal plane bind to the two adjacent layers alternately through covalent bonds, forming a hexagonal crystal with the space group $P63/mcm (D^3_{6h})$. It contains 24 atoms per primitive cell (denoted as Hex- C_{24} hereafter; Figure 1(a) and 1(b)). The formation of interlayer covalent bonds is accompanied by the sp to sp^2 and sp^2 to sp^3 hybridization transition of carbon atoms. In contrast to graphyne, the framework of Hex- C_{24} is composed of sp^2 - and sp^3 -hybridized carbon atoms only without sp -hybridized atoms. The Hex- C_{24} can be thought of as a superlattice of CNTs and graphene nanoribbons (GNRs). The sp^2 -hybridized atoms form narrow GNRs with armchair-shaped edges, while sp^3 -hybridized atoms form ultrathin (3, 0) CNTs (Figure 1(c)). Notably, the (3, 0) CNT in this framework differs significantly from the isolated (3, 0) CNT because the carbon atoms in the former are sp^3 -hybridized.

Structural optimization of the conventional unit cell containing 24 atoms gives the lattice constants of $a = b = 6.826 \text{ \AA}$ and $c = 4.173 \text{ \AA}$. The two nonequivalent carbon atoms occupy the 12k (0.000, 0.215, 0.936) and 12k (0.000, 0.412, 0.413) Wyckoff positions. The density of this Hex- C_{24} (2.84 g cm^{-3}) is between graphite (2.06 g cm^{-3}) and diamond (3.62 g cm^{-3}). Obviously, Hex- C_{24} is a porous material and the

interstitial sites could accommodate other species such as hydrogen and alkali metals and thus holds great promise as a shape-selective catalyst, molecular sieves, and absorbents⁵².

Interestingly, the Hex-C₂₄ is more energetically favorable than graphyne by about 0.36 eV atom⁻¹ (Table 1 and Figure 2(a)). The cohesive energy of the Hex-C₂₄ is even comparable to those of diamond and bct C₄ at zero pressure. Compared with graphyne, Hex-C₂₄ is free from *sp*-hybridized atoms instead of *sp*³-hybridized carbon atoms. Therefore, it is not surprising that the Hex-C₂₄ is energetically advantageous over graphyne. The length of the *sp*²-*sp*² bonds in the center part of GNR component of Hex-C₂₄ is about 1.40 Å, which is very close to graphene's value of 1.42 Å, whereas that of the *sp*²-*sp*² bonds in the armchair edges is shorten to about 1.36 Å. The shrinking of edge bonds have been reported for isolated GNRs with armchair edges⁵⁶. The length of the *sp*³-*sp*³ bonds in the CNT component is 1.56 Å, which is comparable to diamond's value of 1.53 Å. The length of the *sp*²-*sp*³ bonds connecting CNTs and GNR is 1.50 Å. The bond angles deviate slightly from the corresponding standard values of diamond (109.5°) and graphene (120°). The stability of the Hex-C₂₄ is also checked by computing the phonon dispersion along the high-symmetric orientations in the Brillouin zone. We adopted a linear-response theory in the framework of DFT to calculate the phonon spectrum of Hex-C₂₄ as shown in Figure 2(b). No imaginary frequencies are observed in the phonon spectrum confirming the dynamic stability of this novel carbon allotrope.

The Hex-C₂₄ can be obtained from direct compression on multilayer graphyne. We then turned to the structural transition of graphyne to Hex-C₂₄. We referred the previous calculations³¹ and then considered four possible stacking patterns (α , β_1 , β_2 , and β_3) along the z-axis of graphyne film from symmetry considerations using first-principles calculations. However, for β_2 model, when the interlayer distance is 3.65 Å with the pressure of 2 GPa, it transformed into β_1 . In the following calculations, these three models (α , β_1 , and β_3 shown in Figure 3(I)) were adopted as the start point in the transition. Our MEP calculations give a possible pathway for the structural transitions indicated in Figure 3. It is noteworthy that due to the limitation

of the LST/QST strategy implemented in the present DMol3 package that the lattice constants are fixed during the TS searching processes, we employed compressed graphynes and stretched Hex-C₂₄ with identical lattice constants as two adjacent intermediate states as shown in Figure 3(II) and (IV) to search for TS configurations. This roughly mimics the transition processes at different pressure through varying the lattice constants. Recently, a generalized solid-state nudged elastic band (G-SSNEB) method has been presented for determining reaction pathways of solid-solid transformation involving both atomic and unit-cell degrees of freedom⁵⁷. Further studies are therefore needed in future to find the activation pathways between graphyne film and Hex-C₂₄ within a larger configuration space using this effective method. The present calculations, however, give the upper limits of the energy barriers, due to the fixed lattice constants.

For all the three models, the structural transitions have one common property: there are three stages in the process of transformation. The interlayer spaces are first compressed gradually. Sliding and rotating motions between the adjacent layers also take place a little during this stage, but the hybridization of carbon atoms in graphyne is preserved. For these three stacking models, the interlayer distances were set to be identical to 2.60 Å, which correspond to a uniaxial pressure of 34, 26, and 25 GPa along the z-direction (Figure 3(II)). As these are achieved, the graphyne layers begin buckling and bind together. We have obtained these TSs along the transition pathway as shown in Figure 3(III). No TS is found for α model, which means that the critical α state can transform into a stable Hex-C₂₄ phase with a little pressure. For β_1 and β_3 , TSs have features characteristic of AB stacking mode except the buckling. Driven by the interlayer covalent bonds, graphyne layers slide to form AA stacking sequences as shown in Figure 3(IV). And finally convert to stable Hex-C₂₄ phase (Figure 3(V)). The global energy barriers along the pathway measured from the start point to the TSs are only 0.21 eV atom⁻¹ for the three processes, corresponding to the energy barriers at zero pressure. However, measured from the initial configurations at the pressure of 34, 26, and 25 GPa, the energy barriers are 0, 0.04, and 0.04 eV atom⁻¹, respectively. These values are lower than the energy barrier in the transition of graphite to diamond

at high pressure (around $0.15 \text{ eV atom}^{-1}$)^{6, 37, 38}. The low energy barrier of the transition of graphyne to Hex-C₂₄ is related to the high chemical potential of the *sp*-hybridized atoms in graphyne, which makes the *sp-sp*² hybridization transition occur easily. Additionally, the phase transition of graphyne to Hex-C₂₄ is an exothermic process while those of graphite to diamond or other compressed phases are endothermic^{5, 7, 20}. The low energy barrier and the exothermic features of the graphyne-Hex-C₂₄ transition imply that the fabrication of the Hex-C₂₄ from graphyne may be achieved under less rigorous conditions than that of the graphite-diamond transition.

The mechanical and electronic properties of the unique framework of Hex-C₂₄ are quite interesting because whatever the graphyne, (3, 0) CNT or the GNR components have been predicted to have fascinating properties due to their quantum confinement effects. For example, the intersheet adhesion and out-of-plane bending stiffnesses of graphyne are comparable to graphene, despite the density of graphyne being only one-half of that of graphene⁵⁸. CNTs have high stiffness along the axial direction but flexibility in the radial direction, while GNRs possess high stiffness in both radial and axial directions⁵⁹. We evaluated the elastic constants and elastic modulus of Hex-C₂₄ and present them in Table 2. The corresponding values of diamond were also calculated for comparison. The number of independent elastic constants is related to the structure symmetry of materials. The Hex-C₂₄ has five independent elastic constants: C_{11} , C_{33} , C_{44} , C_{12} , and C_{13} . From Table 2, it is obvious that these elastic constants satisfy the mechanical stability conditions for hexagonal crystal: $C_{44} > 0$, $C_{11} > C_{12}$, $(C_{11} + 2C_{12}) \times C_{33} > 2C_{13}^2$. The mechanical stability implies the plausibility of the Hex-C₂₄ from another point.

The elastic constants and modulus of the Hex-C₂₄ exhibit clear anisotropy. Along the z-direction (axial-direction of the two components) the elastic constant (C_{33}) and the Young's modulus (Y_z) are comparable to the corresponding values of diamond, while along the radial directions (x- and y-direction), the Young's moduli are about half the diamond value. We also evaluated the bulk modulus (B) and shear modulus (G) on the basis of elastic constants using Voigt-Reuss-Hill (VRH) approximations⁶⁰

(see Table 2). Based on these values, we evaluated the Vickers hardness (H_v) using two different empirical models as follows:

(a) Chen *et al.* model: ⁶¹

In this model, the hardness of polycrystalline materials is correlated with the shear modulus (G) and bulk modulus (B) by the formula $H_v = 2(k^2G)^{0.585} - 3$, where $k = G/B$ is the Pugh's modulus ratio ⁶². The hardness of Hex-C₂₄ given by using this formula is 44.54 GPa.

(b) Gao *et al.* model: ⁶³

$$H_v = 350 \times N_e^{2/3} \times e^{-1.191f_i} / d^{2.5}$$

The formula correlates the Vickers hardness with the electron density (N_e) of valence electrons per Å³, the ionicity of the chemical bond (f_i) in the crystal on Phillips scale, and the bond length (d). It has been widely used in the calculations of the H_v of crystals. Using this model, the H_v values of the carbon allotrope is estimated to be 91.66 GPa, which is comparable to diamond crystal.

Most researchers agree on the definition according to which “superhard” materials are those with H_v exceeding 40 GPa ⁶⁵. Although there are notable differences between the results of the two empirical models, both of them exceed 40 GPa, suggesting that Hex-C₂₄ is a super-hard material. Recent works ^{55, 66}, have showed that the Gao's model overestimated the H_v of extremely anisotropic compound. We therefore deduce that the hardness of Hex-C₂₄ should be approximately 44.54 to 91.66 GPa, close to the value of c-BN crystal (64.50 GPa) ⁶³.

A useful concept for understanding high mechanical strength is based on the ideal strengths, which represents the maximum stress required to break a perfect crystal ^{67, 68}. Our calculations showed that the ideal tensile strength of diamond along the [111] direction is 90.91 GPa, in good agreement with previous literatures ^{6, 65, 69}. Using the same strategy, we evaluated the ideal tensile strengths of Hex-C₂₄ along the [10 $\bar{1}$ 0], [$\bar{1}$ 2 $\bar{1}$ 0], and [0001] directions, as shown in Figure.4. The corresponding tensile stresses are found to be 75.50, 68.50 and 79.60 GPa at strains of 0.19, 0.18, and 0.14, respectively. The sp^2 - sp^3 bonds connecting CNTs and GNR is more vulnerable to rupture than the sp^3 - sp^3 bonds in the CNT component and the sp^2 - sp^2 bonds in the

GNR component, although it has a shorter bond length (0.06 shorter) than the sp^3 - sp^3 bond. Clearly, along the radial directions in the (0001) surface, Hex- C_{24} has the lowest ideal tensile strength of 68.50 GPa at a strain of 0.18, similar to the cases of monolayer graphyne along the zigzag direction⁵⁸. The shear strength in the (0001)[10 $\bar{1}$ 0] and ($\bar{2}$ 110)[10 $\bar{1}$ 0] slip system are 57.00 and 51.70 GPa with the strains of 0.20 and 0.29, respectively. All these results are consistent with the high H_v values evaluated from the two empirical models.

The covalent bonds between the sp^2 - and sp^3 -hybridized carbon atoms behave differently under stress. Tetrahedral sp^3 -hybridized bonds cannot tolerate large deformations and will abruptly decompose with stress, whereas sp^2 -hybridized bonds can sustain large distortions through out-of-plane bending. Consequently, diamond composed purely of sp^3 -hybridized carbon atoms is extremely brittle, while graphene and graphite formed by sp^2 -hybridized carbon atoms are more ductile. The ductility of the Hex- C_{24} consisting of sp^2 - and sp^3 -hybridized carbon atoms is therefore quite interesting. Here, we adopted a so-called Pugh modulus ratio k ($=G/B$)⁶² as a quantitative criterion for determining the ductile or brittle nature of this novel carbon structure. When k is less than 0.57, the material is regarded as a ductile material, otherwise it is brittle⁶². Our calculations show the k value of Hex- C_{24} is 0.88, indicating that Hex- C_{24} is brittle. We attribute the brittleness to the sp^3 - sp^3 covalent bonds orientating along the z-direction. The high hardness and brittleness of this carbon material with a suitable density, would have wide industrial applications including as abrasives and aerospace materials.

Finally, we turned to the electronic structure of the Hex- C_{24} . The electronic band lines of the Hex- C_{24} obtained from the DFT calculations within PBE functional are plotted in Figure 5(a). Obviously, Hex- C_{24} has the metallic nature at equilibrium. Several bands cross the Fermi level, resulting in electron density of states of 0.12 states eV^{-1} at the Fermi level. The PDOS projected onto the two carbon atoms (C1 and C2 as labeled in Figure 1(a)) are shown in Figure 5(b). It is clear that the electronic states in proximity of the Fermi level come mainly from the 2p orbitals of the sp^2 -hybridized carbon atoms in the GNR component, whereas the contribution from

the sp^3 -hybridized carbon atoms is very small. The carrier velocity from the K point to the H point in the Brillouin zone can be calculated from the formula $\bar{v} = \frac{1}{\hbar} \frac{dE}{dk}$ (E is the energy and k is the wavevector), which can reach the $0.67 \times 10^6 \text{ m s}^{-1}$. This value is very close to that of graphene which is $0.86 \times 10^6 \text{ m s}^{-1}$ from the present calculations. The direction from K point to the H point in the reciprocal space corresponds to axial direction of the GNR component in the real space. It means that the Hex-C₂₄ crystal may be able to conduct anisotropically. The metallic property of Hex-C₂₄ derived chiefly from the sp^2 -hybridized carbon atoms in the GNR component, while it is almost insulating along the radial direction. These features can also be visualized by the isosurfaces of the Kohn–Sham wavefunctions of the $-0.6 \sim 0.2 \text{ eV}$ near the Fermi surface of Hex-C₂₄ in Figure 6. The spatial distribution of the wavefunction implies that Hex-C₂₄ has channels for carriers moving along the axial direction (z-direction), whereas the conductivity is interrupted in the radial direction. Moreover, the electron band lines near the Fermi level are dominated by the π interactions between sp^2 -hybridized carbon atoms. The band lines due to the sp^3 -hybridized carbon atoms are away from the Fermi level. The conductivity of the Hex-C₂₄ is contrast to the most superhard carbon materials which are either insulating or semiconducting and thus is quite promising for the device applications in extremely conditions.

4. Conclusions

From first-principles calculations, we propose a novel carbon allotrope (Hex-C₂₄) composing of sp^2 - and sp^3 -hybridized carbon atoms. It can be synthesized by compressing graphyne film under high pressure. Our calculations imply that the critical pressure is less than 34 GPa and the energy barrier is less than $0.04 \text{ eV atom}^{-1}$. It is energetically more favorable than the parent graphyne by about $0.36 \text{ eV atom}^{-1}$ at zero pressure. The mechanical and dynamic stability of Hex-C₂₄ has also been unambiguously confirmed by the elastic constants and phonon spectrum calculations. The hardness of the Hex-C₂₄ was estimated to be 44.54 – 91.66 GPa, which exceeds 1/2 of diamond, and the ideal tensile strengths and shear strength along highly

symmetric directions are higher than 68.50 and 51.70 GPa, respectively. More interestingly, the superhard Hex-C₂₄ is metallic with several bands across the Fermi level and dispersive electron wavefunction along the axial direction, arising from the *sp*²-hybridized carbon atoms. The void framework, super-hardness, and metallicity make Hex-C₂₄ quite attractive for the applications such as hydrogen storage, advanced abrasives and electronic devices working at extremely conditions.

Acknowledgements

This work is supported by the National Basic Research Program of China (No. 2012CB932302), the National Natural Science Foundation of China (No.91221101), the Natural Science Fund for Distinguished Young Scholars of Shandong Province (No. JQ201001), and the research projects of Shandong University of Traditional Chinese Medicine (No. ZYDXY1356).

References

- 1 M. S. Dresselhaus, G. Dresselhaus, and P. C. Eklund, *Academic press, San Diego, CA*, 1996, 965.
- 2 S. Chen, X. G. Gong and S.-H. Wei, *Phys. Rev. Lett.*, 2007, **98**, 015502.
- 3 Q. Li, Y. Sun, Z. Li and Y. Zhou., *Scripta Mater.*, 2011, **65**, 229.
- 4 Q. Li, Y. Ma, A. R. Oganov, H. Wang, H. Wang, Y. Xu, T. Cui, H.-K. Mao and G. Zou, *Phys. Rev. Lett.*, 2009, **102**, 175506.
- 5 K. Umemoto, R. M. Wentzcovitch, S. Saito and T. Miyake, *Phys. Rev. Lett.*, 2010, **104**, 125504.
- 6 X.-F. Zhou, G.-R. Qian, X. Dong, L. Zhang, Y. Tian and H.-T. Wang, *Phys. Rev. B*, 2010, **82**, 134126.
- 7 J.-T. Wang, C. Chen and Y. Kawazoe, *Phys. Rev. Lett.*, 2011, **106**, 075501.
- 8 M. Amsler, J. A. Flores-Livas, L. Lehtovaara, F. Balima, S. A. Ghasemi, D. Machon, S. Pailhès, A. Willand, D. Caliste, S. Botti, A. S. Miguel, S. Goedecker and M. A. L. Marques, *Phys. Rev. Lett.*, 2012, **108**, 065501.
- 9 Z. Li, F. Gao and Z. Xu, *Phys. Rev. B*, 2012, **85**, 144115.
- 10 H. Niu, X.-Q. Chen, S. Wang, D. Li, W. L. Mao, and Y. Li, *Phys. Rev. Lett.*, 2012, **108**, 135501.
- 11 Q. Zhu, Q. Zeng, and A. R. Oganov, *Phys. Rev. B*, 2012, **85**, 201407.
- 12 Y. Liang, W. Zhang and L. Chen, *EPL (Europhysics Letters)*, 2009, **87**, 56003.
- 13 C. J. Pickarda, V. Milman and Björn Winkler, *Diam. Relat. Mater.*, 2001, **10**, 2225..
- 14 Y. Liang, W. Zhang, J. Zhao and L. Chen, *Phys. Rev. B*, 2009, **80**, 113401.
- 15 W. Luo and W. Windl, *Carbon*, 2009, **47**, 367.
- 16 H. W. Kroto, J. R. Heath, S. C. O'Brien, R. F. Curl and R. E. Smalley, *Nature*, 1985, **318**, 162.
- 17 S. Iijima, *Nature*, 1991, **354**, 56.
- 18 K. S. Novoselov, A. K. Geim, S. V. Morozov, D. Jiang, Y. Zhang, S. V. Dubonos,

- I. V. Grigorieva and A. A. Firsov, *Science*, 2004, **306**, 666.
- 19 N. Narita, S. Nagai, S. Suzuki and K. Nakao, *Phys. Rev. B*, 1998, **58**, 11009.
- 20 Z. Zhao, B. Xu, X.-F. Zhou, L.-M. Wang, B. Wen, J. He, Z. Liu, H.-T. Wang and Y. Tian, *Phys. Rev. Lett.*, 2011, **107**, 215502.
- 21 WL. Mao, HK. Mao, PJ. Eng, TP. Trainor, M. Newville, CC. Kao, DL. Heinz, JF. Shu, Y. Meng and RJ. Hemley, *Science* 2003, **302**, 425
- 22 Y. Iwasa, T. Arima, R. M. Fleming, T. Siegrist, O. Zhou, R. C. Haddon, L. J. Rothberg, K. B. Lyons, H. L. Carter Jr., A. F. Hebard, R. Tycko, G. Dabbagh, J. J. Krajewski, G. A. Thomas and T. Yagi, *Science*, 1994, **264**, 1570.
- 23 V. D. Blank, S. G. Buga, N. R. Serebryanaya, G. A. Dubitsky, B. N. Mavrin, M. Yu. Popov, R. H. Bagramov, V. M. Prokhorov, S. N. Sulyanov, B. A. Kulnitskiy and Y.V. Tatyaniin, *Carbon*, 1998, **36**, 665.
- 24 R. S. Kumar, M. G. Pravica, A. L. Cornelius, M. F. Nicol, M. Y. Hu and P. C. Chow, *Diam. Relat. Mater.*, 2007, **16**, 1250.
- 25 W. Guo, C. Z. Zhu, T. X. Yu, C. H. Woo, B. Zhang and Y. T. Dai, *Phys. Rev. Lett.*, 2004, **93**, 245502.
- 26 Z. Wang, Y. Zhao, K. Tait, X. Liao, D. Schiferl, C. Zha, R. T. Downs, J. Qian, Y. Zhu and T. Shen, *PNAS*, 2004, **101**, 13699.
- 27 M. Popov, M. Kyotani and Y. Koga, *Diam. Relat. Mater.*, 2003, **12**, 833.
- 28 M. Hu, Z. Zhao, F. Tian, A. R. Oganov, Q. Wang, M. Xiong, C. Fan, B. Wen, J. He, D. Yu, H.-T. Wang, B. Xu and Y. Tian, *Sci. Rep.*, 2013, **3**, 1331.
- 29 Y. Lin, L. Zhang, H.-k. Mao, P. Chow, Y. Xiao, M. Baldini, J. Shu and W. L. Mao, *Phys. Rev. Lett.*, 2011, **107**, 175504.
- 30 N. Narita, S. Nagai, S. Suzuki and K. Nakao, *Phys. Rev. B*, 2000, **62**, 11146.
- 31 M. K. Joshua, H. K. James, J. E. Jamieson, A. J. Charles, C. P. Ryan and M. H., Michael, *Org. Lett.*, 2000, **2**, 969.
- 32 Y. Takashi, I. Akiko, S. Motohiro, T. Kazukuni, T. Yoshito and V. W. Richard, *Org. Lett.*, 2006, **8**, 2933.
- 33 C. A. Johnson, Y. Lu and M. M. Haley, *Org. Lett.*, 2007, **9**, 3725.
- 34 M. M. Haley, *Pure Appl. Chem.*, 2008, **80**, 519.

- 35 G. Li, Y. Li, H. Liu, Y. Guo, Y. Li and D. Zhu, *Chem. Commun.*, 2010, **46**, 3256.
- 36 A. N. Enyashin and A. L. Ivanovskii, *phys. status solidi B*, 2011, **248**, 1879.
- 37 P. Xiao and G. Henkelman, *J. Chem. Phys.*, 2012, **137**, 101101.
- 38 Salah Eddine Boulfefel, Artem R. Oganov and Stefano Leoni, *Sci. Rep.*, 2012, **2**, 471.
- 39 M D Segall, P. J D Lindan, M J Probert, C J Pickard, P J Hasnip, S J Clark and M C Payne, *J. Phys.: Condens. Matter*, 2002, **14**, 2717.
- 40 J. P. Perdew, K. Burke and M. Ernzerhof, *Phys. Rev. Lett.*, 1996, **77**, 3865.
- 41 H. J. Monkhorst and J. D. Pack, *Phys. Rev. B*, 1976, **13**, 5188.
- 42 B. G. Pfrommer, M. Côté, S. G. Louie and M. L. Cohen, *J. Comput. Phys.*, 1997, **131**, 233.
- 43 T. A. Halgren and W. N. Lipscomb, *Chem. Phys. Lett.*, 1977, **49**, 225.
- 44 B. Delley, *J. Chem. Phys.*, 1990, **92**, 508.
- 45 B. Delley, *J. Chem. Phys.*, 2000, **113**, 7756.
- 46 G. Henkelman and H. Jónsson, *J. Chem. Phys.*, 2000, **113**, 9978.
- 47 K. Parlinski, Z. Q. Li and Y. Kawazoe, *Phys. Rev. Lett.*, 1997, **78**, 4063.
- 48 G. Kresse and J. Furthmüller, *Phys. Rev. B*, 1996, **54**, 11169.
- 49 G. Kresse and J. Furthmüller, *Comp. Mater. Sci.*, 1996, **6**, 15.
- 50 C. Kittel, *John Wiley & Sons, New York*, 1996.
- 51 J. Furthmüller, J. Hafner and G. Kresse, *Phys. Rev. B*, 1994, **50**, 15606.
- 52 Z. Zhao, B. Xu, L.-M. Wang, X.-F. Zhou, J. He, Z. Liu, H.-T. Wang and Y. Tian, *ACS Nano*, 2011, **5**, 7226.
- 53 X.-L. Sheng, Q.-B. Yan, F. Ye, Q.-R. Zheng and G. Su, *Phys. Rev. Lett.*, 2011, **106**, 155703.
- 54 H. Bu, M. Zhao, A. Wang and X. Wang, *Carbon*, 2013, **65**, 341.
- 55 H. Bu, M. Zhao, Y. Xi, X. Wang, H. Peng, C. Wang and X. Liu, *EPL (Europhysics Letters)*, 2012, **100**, 56003.
- 56 Y.-W. Son, M. L. Cohen and S. G. Louie, *Phys. Rev. Lett.*, 2006, **97**, 216803.
- 57 D. Sheppard, P. Xiao, W. Chemelewski, D. D. Johnson, and Graeme Henkelman, *J. Chem. Phys.*, 2012, **136**, 074103.

- 58 S. W. Cranford and M. J. Buehler, *Carbon*, 2011, **49**, 4111.
- 59 R. Faccio, P. A. Denis, H. Pardo, C. Goyenola and Á. W. Mombrú, *J. Phys.: Condens. Mat.*, 2009, **21**, 285304.
- 60 R. Hill, *Proc. Phys. Soc. A*, 1952, **65**, 349.
- 61 X.-Q. Chen, H. Niu, D. Li and Y. Li, *Intermetallics*, 2011, **19**, 1275.
- 62 S. F. Pugh, *Philos. Mag.*, 1954, **45**, 823.
- 63 F. Gao, J. He, E. Wu, S. Liu, D. Yu, D. Li, S. Zhang and Y. Tian, *Phys. Rev. Lett.* , 2003, **91**, 015502.
- 64 H. Yao, L. Ouyang and W.-Y. Ching, *J. Am. Ceram. Soc.*, 2007, **90**, 3194.
- 65 J. Qin, D. He, J. Wang, L. Fang, L. Lei, Y. Li, J. Hu, Z. Kou and Y. Bi, *Adv. Mater.*, 2008, **20**, 4780.
- 66 X.-Q. Chen, H. Niu, C. Franchini, D. Li and Y. Li, *Phys. Rev. B*, 2011, **84**, 121405.
- 67 Y. Zhang, H. Sun and C. Chen, *Phys. Rev. Lett.*, 2004, **93**, 195504.
- 68 D. Roundy and M. L. Cohen, *Phys. Rev. B*, 2001, **64**, 212103.
- 69 H. Chacham and L. Kleinman, *Phys. Rev. Lett*, 2000, **85**, 4904.

Figure captions

Figure 1 (color online) Atomic structure of Hex-C₂₄ composing of sp^2 - and sp^3 -hybridized carbon atoms. (a) Top view, (b) Side view, (c) Schematic representation of the superlattice of (3, 0) CNTs and GNRs.

Figure 2 (color online) (a) The total energy per atom of carbon allotropes as a function of atomic density. The total energies of T-carbon⁵³, h-carbon⁵⁴ and yne-diamond⁵⁵ proposed in previous works are also presented for purpose of comparison. (b) Phonon band structure of Hex-C₂₄.

Figure 3 (color online) A possible pathway of the structural transition of graphyne to Hex-C₂₄. The energy of the product (Hex-C₂₄) is set to zero and the numbers in parentheses are the energy referenced to the product (eV atom⁻¹). I (reactant), II (critical state), III (TS), IV(intermediate) and V(product) columns show the key states in the reaction process. (a), (b), and (c) rows show the transition processes of α , β_1 , and β_3 structure.

Figure 4 (color online) The orientation-dependent stress-strain relations for the tensile and shear deformation in Hex-C₂₄.

Figure 5 (color online) (a) The electronic band structures of Hex-C₂₄ along high symmetry direction in Brillouin zone. (b) The electron density of states (PDOS) projected onto the s- and p-orbitals of the carbon atoms with different hybridization (C1, and C2 as labeled in Figure 1(a)). The energy at the Fermi level was set to zero.

All the results were obtained from the DFT calculations within PBE functional.

Figure 6 (color online) The isosurfaces of the Kohn-Sham wavefunctions of -0.6 ~ 0.2

eV near the Fermi surface of Hex-C₂₄. The energy at the Fermi level was set to 0 and the isovalue was set to 0.006 Å^{-3/2}. Top and side views are plotted in the left and right columns.

Table captions

Table 1. The crystal system (system), space groups (groups), equilibrium density ρ (g cm^{-3}), cohesive energy E_{coh} (eV atom^{-1}), energy band gap E_g (eV), of diamond, graphite, graphdiyne, graphyne, T-carbon, bct C_4 , and Hex- C_{24} at zero pressure.

Table 2. The calculated elastic constants (C_{11} , C_{22} , C_{33} , C_{44} , C_{55} , C_{66} , C_{12} , C_{13} , C_{14} and C_{23}), Young's modulus (Y_x , Y_y , and Y_z), bulk modulus (B), shear modulus (G), hardness(H_v) and Pugh modulus (k) of diamond and Hex- C_{24} . The units of these parameters except Pugh modulus are GPa . Noting that for diamond with cubic lattice, there are only four independent elastic constants.

Table 1. The crystal system (system), space groups (groups), equilibrium density ρ (g cm^{-3}), cohesive energy E_{coh} (eV atom^{-1}), energy band gap E_g (eV), of diamond, graphite, graphdiyne, graphyne, T-carbon, bct C_4 , and Hex- C_{24} at zero pressure.

| | | system | groups | ρ | E_{coh} | E_g |
|---------------|-------------------|--------|----------------|-------------|-----------|-------|
| diamond | Our | Cub | Fd $\bar{3}m$ | 3.62 | 8.20 | 4.40 |
| | Ref. ^a | | 227 | 3.52 | 7.37 | 5.45 |
| graphite | Our | Hex | P6/mmm | 2.06 | 8.35 | -- |
| | Ref. ^b | | 191 | ~ 2.27 | 7.37 | -- |
| graphdiyne | Our | Hex | P6/mmm | -- | 7.65 | 0.53 |
| | | | 191 | | | |
| graphyne | Our | Hex | P6/mmm | -- | 7.77 | 0.47 |
| | | | 191 | | | |
| T-carbon | Our | Cub | Fd $\bar{3}m$ | 1.56 | 7.05 | 2.12 |
| | | | 227 | | | |
| bct C_4 | Our | Tetra | I4/mmm | 3.42 | 7.99 | 3.71 |
| | | | 139 | | | |
| Hex- C_{24} | Our | Hex | P63/mcm 193 | 2.84 | 8.13 | -- |

^a Reference 50.

^b Reference 51.

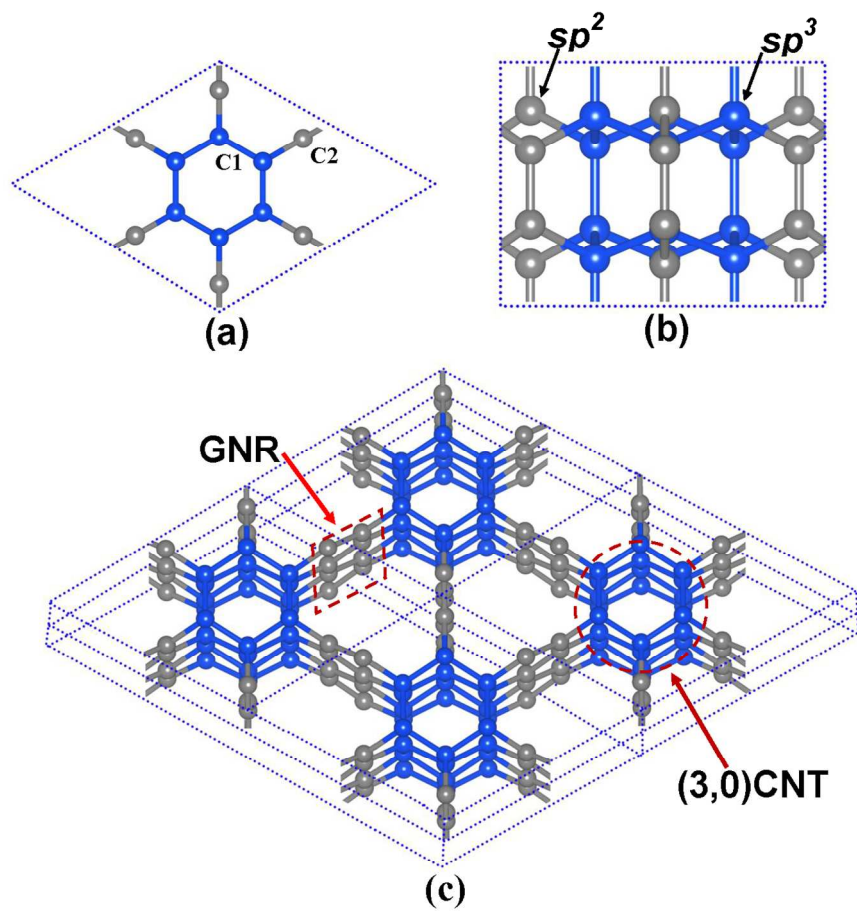
Table 2. The calculated elastic constants (C_{11} , C_{22} , C_{33} , C_{44} , C_{55} , C_{66} , C_{12} , C_{13} , C_{14} and C_{23}), Young's modulus (Y_x , Y_y , and Y_z), bulk modulus (B), shear modulus (G), hardness(H_v) and Pugh modulus (k) of diamond and Hex-C₂₄. The units of these parameters except Pugh modulus are *GPa*. Noting that for diamond with cubic lattice, there are only four independent elastic constants.

| | Diamond | Hex-C₂₄ |
|----------|------------------------|--|
| | Our/Refs. ^a | |
| C_{11} | 1085.45/1079 | 609.03 |
| C_{33} | -- | 1102.69 |
| C_{44} | 582.11/578 | 325.78 |
| C_{12} | 113.39/124 | 188.88 |
| C_{13} | -- | 82.77 |
| Y_x | 1064.00/1063 | 547.47 |
| Y_y | -- | 547.47 |
| Y_z | -- | 1085.52 |
| B | 437.41/442 | 330.38 |
| G | 541.55/ 536 | 290.67 |
| H_v | 99.03/96±5 | 44.54 ^b /91.66 ^c |
| k | 1.24/1.21 | 0.88 |

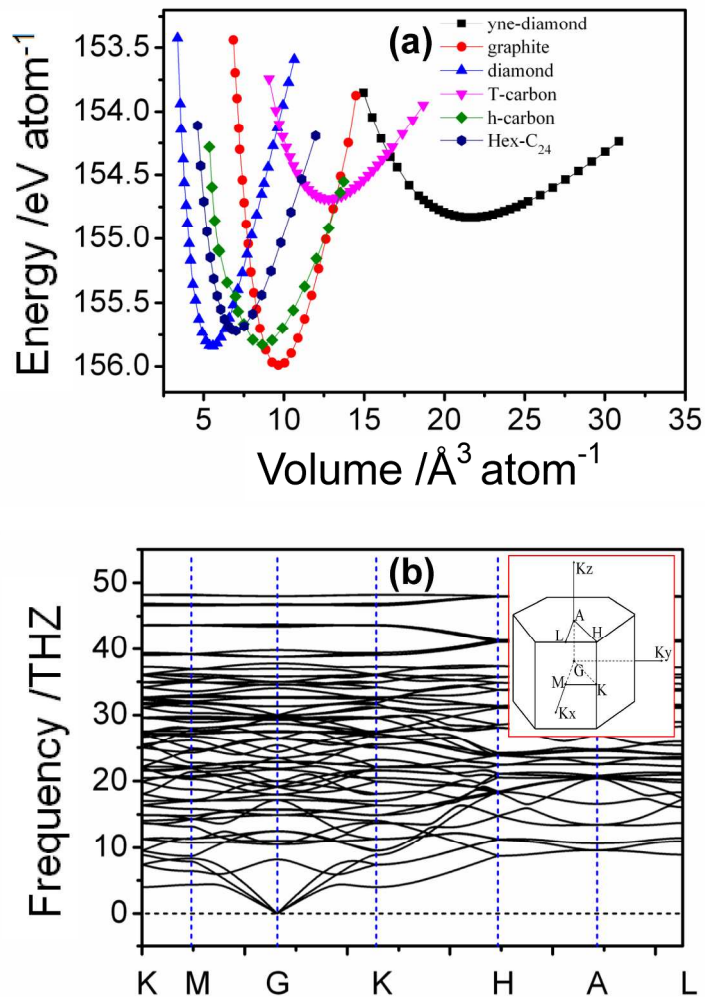
^a Reference 63, 64.

^b Chen's result.

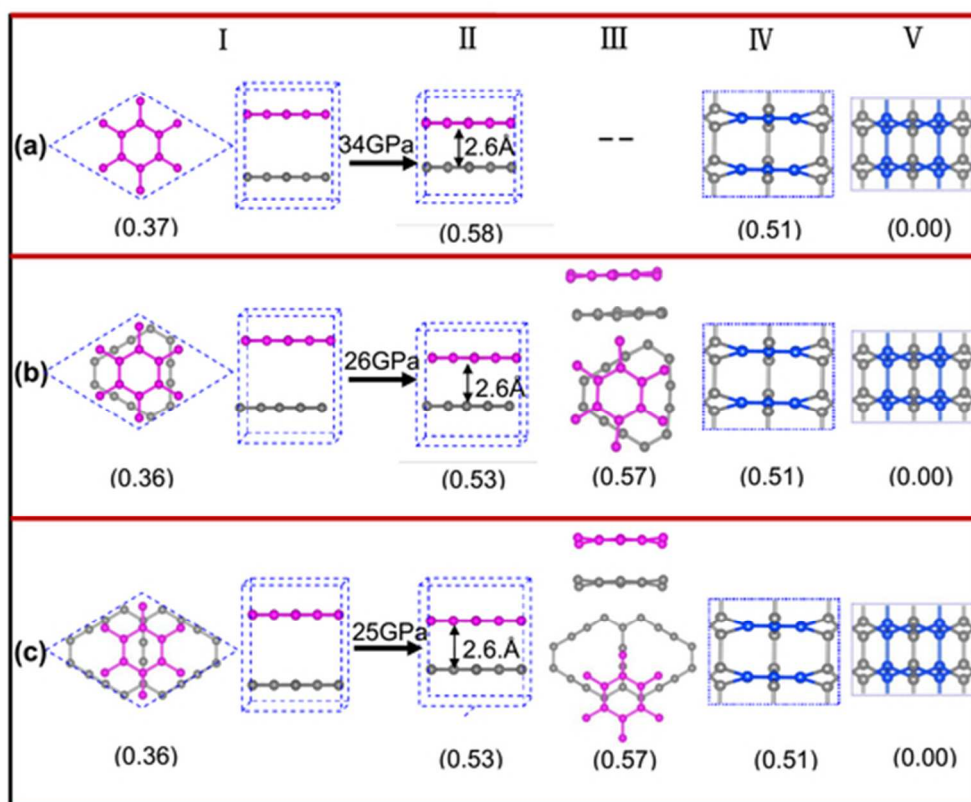
^c Gao's result.



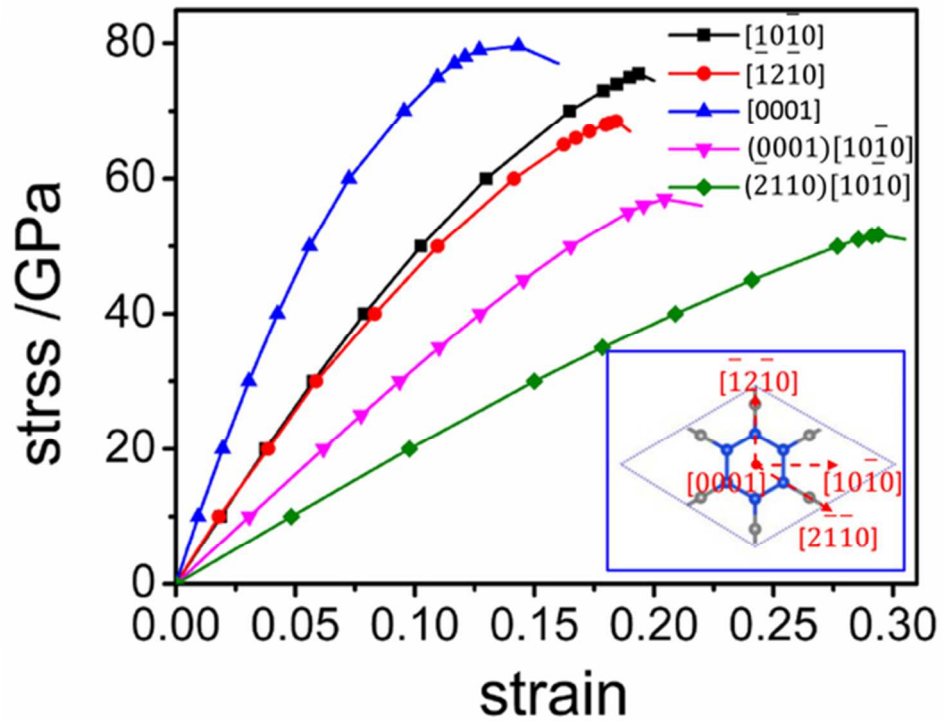
Atomic structure of Hex-C24 composing of sp^2 - and sp^3 -hybridized carbon atoms. (a) Top view, (b) Side view, (c) Schematic representation of the superlattice of (3, 0) CNTs and GNRs.
214x218mm (300 x 300 DPI)



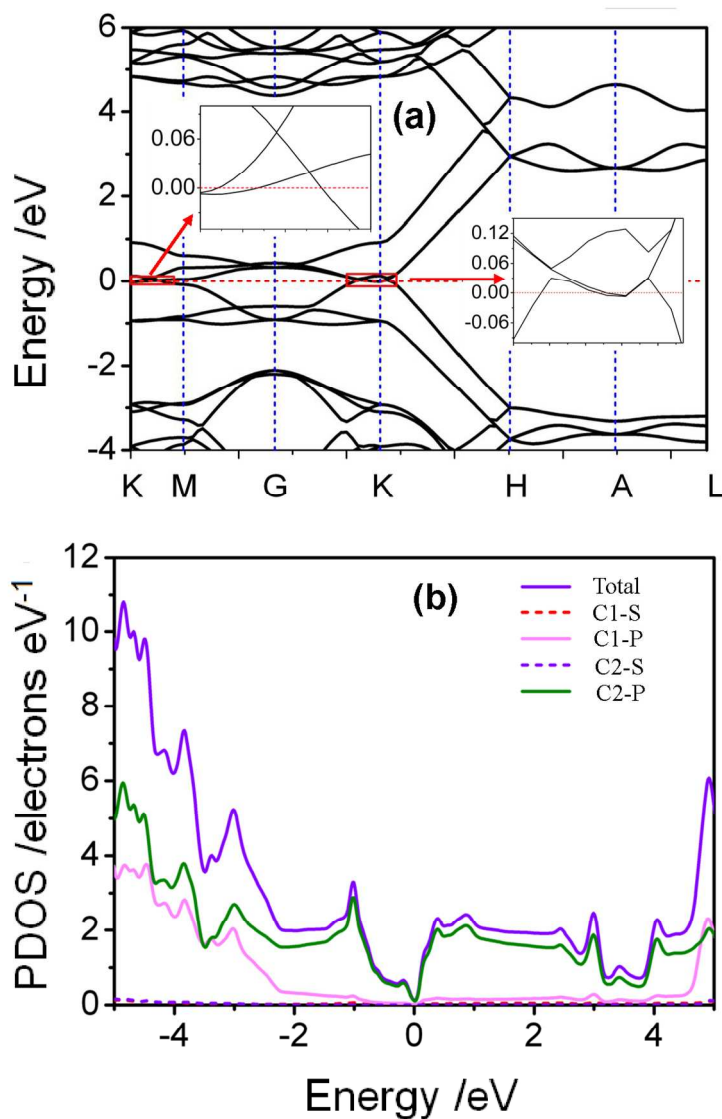
(a) The total energy per atom of carbon allotropes as a function of atomic density. The total energies of T-carbon 53, h-carbon 54 and yne-diamond 55 proposed in previous works are also presented for purpose of comparison. (b) Phonon band structure of Hex-C₂₄.
236x266mm (300 x 300 DPI)



A possible pathway of the structural transition of graphyne to Hex-C24. The energy of the product (Hex-C24) is set to zero and the numbers in parentheses are the energy referenced to the product (eV atom⁻¹). I (reactant), II (critical state), III (TS), IV(intermediate) and V(product) columns show the key states in the reaction process. (a), (b), and (c) rows show the transition processes of α , β_1 , and β_3 structure.
47x39mm (300 x 300 DPI)

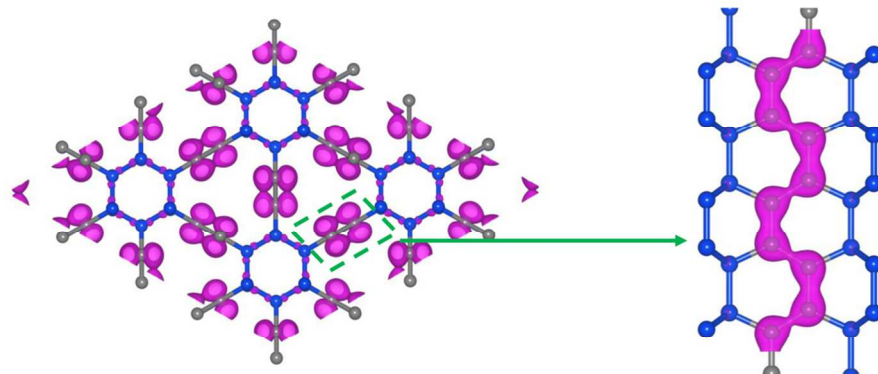


The orientation-dependent stress-strain relations for the tensile and shear deformation in Hex-C24.
51x43mm (300 x 300 DPI)



(a) The electronic band structures of Hex-C24 along high symmetry direction in Brillouin zone. (b) The electron density of states (PDOS) projected onto the s- and p-orbitals of the carbon atoms with different hybridization (C1, and C2 as labeled in Figure 1(a)). The energy at the Fermi level was set to zero. All the results were obtained from the DFT calculations within PBE functional.

246x288mm (300 x 300 DPI)



106x55mm (300 x 300 DPI)

From first-principles calculations, a novel carbon material with superhardness and metallicity is proposed and a possible endothermic transition is evaluated.

